

Nonlinear Optical Diffraction Effects and Solitons due to Anisotropic Charge-Diffusion-Based Self-Interaction

B. Crosignani,¹ A. Degasperis,² E. DelRe,³ P. Di Porto,¹ and A. J. Agranat⁴

¹*Dipartimento di Fisica, Universita' dell'Aquila, 67010 L'Aquila, Italy*

and Istituto Nazionale di Fisica della Materia, Unità di Roma I, Rome, Italy

²*Dipartimento di Fisica, Universita' di Roma "La Sapienza," 00185 Rome, Italy*

and Istituto Nazionale di Fisica Nucleare, Sezione di Roma I, Rome, Italy

³*Fondazione Ugo Bordonis, Via Baldassarre Castiglione 59, 00142 Rome, Italy*

⁴*Department of Applied Physics, Hebrew University of Jerusalem, Israel*

(Received 23 July 1998)

We report the first observation of self-modified optical diffraction, beam ellipticity recovery and conservation, and intensity independent self-focusing in an anisotropic diffusion-type nonlinearity realized in ferroelectrics heated above the centrosymmetric transition. The interaction, a photorefractive diffusion-driven quadratic nonlinearity, constitutes the first known natural realization of a higher-order logarithmic nonlinearity and allows an analytical description of the observed phenomena and the prediction of a class of noncircular solitons with no characteristic length scale. [S0031-9007(99)08475-6]

PACS numbers: 42.65.Hw, 05.45.Yv, 42.65.Tg, 42.70.Nq

Strongly interacting systems and nonlinear dynamics is one of the main subjects of interest in modern physics. In optics, nonlinear propagation has allowed the observation and understanding of a wealth of new phenomena. A detailed description of these processes implies tackling a nonlinear propagation equation whose solution is rarely available for a continuous set of system parameters. In this Letter we investigate experimentally and theoretically, for the first time, nonlinear propagation of a localized optical beam in a ferroelectric heated above the Curie temperature. We observe intensity independent spatial self-focusing and anomalous beam aspect ratio evolution caused by the thermodynamically enhanced photorefractive diffusion nonlinearity. The basic relevant physical model, common to all standard doped ferroelectrics, produces the first natural realization of a higher-order anisotropic nonlocal logarithmic-type nonlinearity which remarkably allows a direct nonperturbative analytical treatment. The model equation allows the interpretation of the observed phenomena and furthermore supports what is to our knowledge the first class of two-dimensional solitary waves, in the form of noncircular spatial solitons, without a characteristic transverse length scale.

Light propagation in ferroelectrics in the centrosymmetric phase (referred to as paraelectrics) has been shown to support, in a different physical configuration, screening solitons [1,2] and diffusion-driven effects [3]. In the ferroelectric phase, diffusion has been shown to sustain non-diffracting propagation, self-bending, and fanning [4].

Evolution of beam ellipticity (aspect ratio) has been experimentally investigated in quadratic nonlinear media [5], in saturated inhomogeneous broadened resonant media [6], and in Kerr-like and saturated media [7,8].

Our experiments were carried out making use of the setup schematically illustrated in Fig. 1. The first experiment we performed consisted of launching into a sample of

KLTN (potassium-lithium-tantalate-niobate), a perovskite-like ferroelectric, a 1D Gaussian beam, and observing its diffraction at the output facet. The input beam, a TEM₀₀ $\lambda = 515$ nm polarized (along the x direction) beam from a cw argon ion laser, is focused onto the input facet of the sample by means of a cylindrical lens with $f = 150$ mm (and axis parallel to the y direction). The sample of KLTN measures $3.7^{(x)} \times 4.6^{(y)} \times 2.4^{(z)}$ mm, being zero cut and polished along its cubic axes. The crystal is doped with Cu and V impurities and manifests its dielectric anomaly at $T_c = 9.8^\circ\text{C}$ (decreasing temperature loop) passing from the room temperature cubic paraelectric phase to the noncentrosymmetric ferroelectric phase. We monitored input beam profile and output diffraction along the z direction (direction of propagation) by means of an imaging lens ($f = 60$ mm) and a CCD camera. The crystal temperature was controlled via a Peltier junction in thermal contact

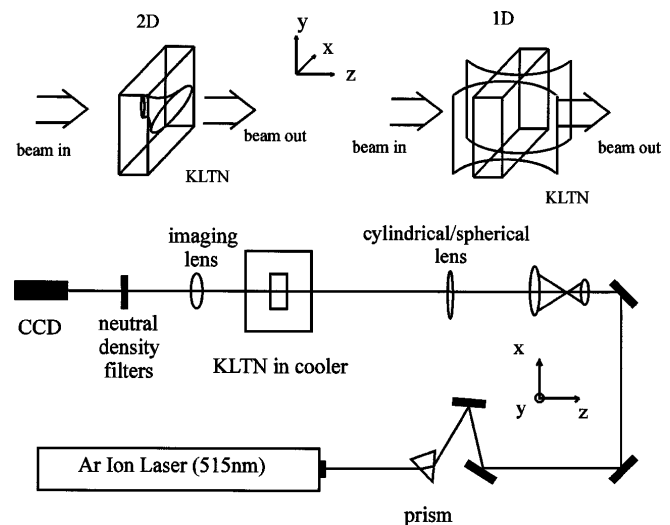


FIG. 1. Experimental setup.

with the crystal. In this configuration the input light distribution (a slab of light) has an input full width at half maximum (FWHM) of $13\ \mu\text{m}$ (in the confined x direction). When the crystal is kept at room temperature ($T_c = 20^\circ\text{C}$) the beam diffracts to $22\ \mu\text{m}$, as expected from linear Gaussian diffraction with a crystal index of refraction $n = 2.4$. Lowering the crystal temperature towards T_c we observed considerable self-focusing as shown in Fig. 2 from 22 to $17\ \mu\text{m}$. At even lower temperatures, as the critical regime was reached, we observed domain formation and strong beam distortion (the first domain nucleation was observed at 10.0 – 10.2°C). Heat transfer occurred only through the bottom facet of the crystal which was therefore not uniformly thermalized during the experiment, presenting a transverse temperature gradient (especially at low values of T). Our observations refer to a limited transverse (in the xy plane) region of the crystal (about $200 \times 200\ \mu\text{m}$), where the effect of the gradient was negligible. The peak beam intensity used was of the order of $I_0 \approx 10^2\ \text{W}/\text{cm}^2$, at the crystal input face (spurious background illumination was at least 4 orders of magnitude less intense). The experiment was repeated for higher values of I_0 (up to 10 times more intense), but no appreciable difference was observed, other than in the duration of the transient buildup regime. Next we investigated $(2 + 1)\text{D}$ propagation in this same configuration. We substituted the cylindrical lens with a spherical one and launched, at the input facet of the crystal, a highly confined circular Gaussian beam. At the output we observed Gaussian linear propagation for room temperature, but as the crystal was cooled into the near-transition regime, we observed a peculiar beam deformation leading to a beam with an elliptical transverse intensity profile. The beam manifested self-focusing in the x direction, parallel to the beam polarization (which did not suffer any rotation). Thus, introducing a prism (as shown in Fig. 1) before the beam expander, we launched an asymmetric elliptical, approximately

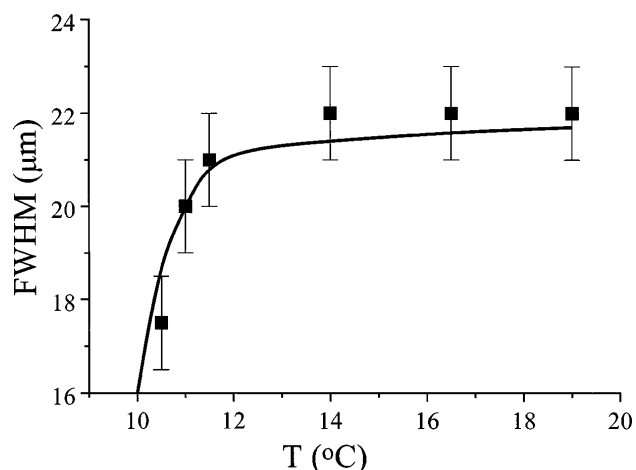


FIG. 2. Output beam FWHM [(1 + 1)D case] compared to theory.

stigmatic, Gaussian beam into the crystal and observed diffraction as a function of temperature. Results are shown in Fig. 3. The input beam, with intensity $\text{FWHM}_x = 7\ \mu\text{m}$ and $\text{FWHM}_y = 11\ \mu\text{m}$, has an input ellipticity $\Lambda = (\text{FWHM}_y/\text{FWHM}_x) = 1.5$. For high values of temperature, at which beam propagation is linear (from approximately 15°C upwards diffusion has a negligible effect), we observed the typical “inversion” of ellipticity at the output of the crystal, from 1.5 to 0.7 , this being a consequence of a standard diffraction (stronger confinement, stronger diffraction). As we lowered the crystal temperature we observed an evolution of the output ellipticity towards a *higher value*. At approximately $T = 10.2^\circ\text{C}$ we recovered the input ellipticity, as shown in Fig. 3, the beam maintaining its Gaussian transverse profile. We adjusted the input laser power in order to have a peak intensity comparable to the $(1 + 1)\text{D}$ case and again repeated the experiment for various values of I_0 observing no appreciable difference in the final stationary configuration.

Optical beams propagating in a doped ferroelectric suffer self-distortion dynamics through the photorefractive diffusion nonlinearity. Above the Curie temperature the local refractive index modulation is induced by the *quadratic* electro-optic response to the light generated diffusion field. The strength of the self-interaction is determined by the magnitude of the diffusion field and crystal response. In particular, for a confined beam with intensity distribution $I(x, y, z)$ (typically an input Gaussian beam) propagating in the z direction, the diffusion field $\mathbf{E}^{(d)} \cong -(K_b T/e)\nabla I(x, y, z)/I(x, y, z)$ [9], independent of the beam peak intensity I_0 , induces via the quadratic Pockels effect a tensorial refractive index change given by $\Delta n_{ij} = -(\frac{1}{2})n^3(\epsilon_0\epsilon_r)^2 g_{ijkl} E_k^{(d)} E_l^{(d)}$, where n is the crystal index of refraction, T is the temperature, g_{ijkl} is the quadratic electro-optic tensor, ϵ_0 is the vacuum dielectric constant, and ϵ_r is the static

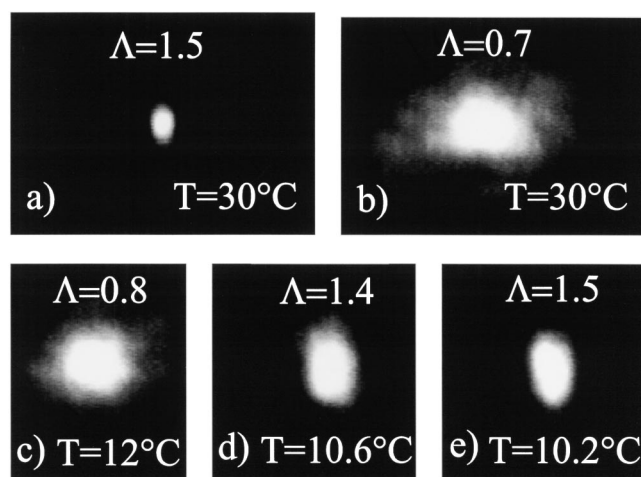


FIG. 3. (a) Input beam at $T = 30^\circ\text{C}$, $\text{FWHM}_{x,y} = (7, 11)\ \mu\text{m}$; (b)–(e): output diffraction, with final $\text{FWHM}_{x,y} = (15, 23)\ \mu\text{m}$.

relative dielectric constant. Limiting our approach to diffusion-driven phenomena for values of T that do not allow for domain formation (our experiments *do not* investigate effects due to domain formation), the local lattice polarization is taken to be $\mathbf{P} = \varepsilon_0 \varepsilon_r \mathbf{E}^{(d)}$ [10]. In this regime, the mean-field Curie-Weiss theory applies and $\varepsilon_r = C/(T - T_0)$, where C and T_0 are phenomenological constants.

The parabolic paraxial equation describing monochromatic propagation is

$$\left[i \frac{\partial}{\partial z} + \frac{1}{2k} \left(\frac{\partial^2}{\partial x^2} + \frac{\partial^2}{\partial y^2} \right) \right] A_i(x, y, z) + \frac{k}{n} \Delta n_{ij} A_j(x, y, z) = 0, \quad (1)$$

where $A(x, y, z)$ is the slowly varying amplitude of the optical field $\mathbf{E}_{\text{opt}} = \mathbf{A}(x, y, z) \exp(ikz - i\omega t) + \text{c.c.}$, and $k = n\omega/c$. Equation (1) assumes a scalar form for a large class of ferroelectrics above the Curie temperature. For example, for perovskite-type compounds (like KLTN), the symmetry is $m3m$ [11], and only two relevant independent electro-optic coefficients, that is $g_{xxx} = g_{11}$ and $g_{xyy} = g_{12}$, are nonzero [12]. This is equally true for symmetry classes $2m$, 222 , mmm , 422 , $4mm$, $42m$, $4/mm$, 23 , $m3$, 432 , and $43m$, if polarization coupling through the g_{xyy} term is again negligible. We limit our analysis to positive values of g_{11} and g_{12} occurring in perovskites (like KLTN), although the treatment can be extended to negative values, in which case defocusing plays an important role. Hence, for an input x -polarized beam, Eq. (1) is reduced to the scalar form,

$$\left[i \frac{\partial}{\partial \xi} + \left(\frac{\partial^2}{\partial \xi^2} + \frac{\partial^2}{\partial \eta^2} \right) \right] A + \left[\gamma_1 \left(\frac{\partial |A|^2 / \partial \xi}{|A|^2} \right)^2 + \gamma_2 \left(\frac{\partial |A|^2 / \partial \eta}{|A|^2} \right)^2 \right] A = 0, \quad (2)$$

where $A = A_x$, $\gamma_1 = -k^2 n^2 \varepsilon_0^2 (\varepsilon_r - 1)^2 g_{11} (K_b T / e)^2$, $\gamma_2 = -k^2 n^2 \varepsilon_0^2 (\varepsilon_r - 1)^2 g_{12} (K_b T / e)^2$, and we have introduced the dimensionless variables $(\xi, \eta) = \sqrt{2}(kx, ky)$, $\zeta = kz$. Equation (2) represents the scalar anisotropic diffusion-driven nonlinear propagation equation. Anisotropy is contained in the fact that, in general, $\gamma_1 \neq \gamma_2$, whereas nonlocality is contained in the derivative in the nonlinear source, typical of any diffusion-based process. The form of the nonlinear term, the square of a logarithmic derivative, allows for a number of explicit solutions, all independent of the beam peak intensity I_0 . We limit our investigation to two classes corresponding, respectively, to nonlinear diffraction and self-trapping. The first one reads

$$A(\xi, \eta, \zeta) = \frac{A_0}{(p_1 p_2)^{1/4}} \exp(-\xi^2/d_1^2 p_1 - \eta^2/d_2^2 p_2) \times \exp[i\phi(\xi, \eta, \zeta)], \quad (3)$$

where $d_{1,2}$ are the input (normalized) widths in the x, y directions, $p_{1,2} = [1 + b_{1,2}(\zeta - \zeta_{1,2})^2]$ with $b_{1,2} =$

$16(1 + 4\gamma_{1,2})/d_{1,2}^4$ and $\phi(\xi, \eta, \zeta) = (p_1' \xi^2/p_1 + p_2' \eta^2/p_2)/8 - (2/d_1^2 b_1^{1/2}) \arctan[b_1^{1/2}(\zeta - \zeta_1)] - (2/d_2^2 b_2^{1/2}) \arctan[b_2^{1/2}(\zeta - \zeta_2)]$ (the prime standing for the derivative with respect to ζ). It is valid for values of $0 > \gamma_{1,2} > -\frac{1}{4}$ and describes nonlinear self-focusing in the two transverse dimensions x and y . When a Gaussian beam is focused onto the $z = 0$ plane, we deduce from Eq. (3) that its ellipticity Λ evolves as

$$\Lambda(\zeta) = \frac{d_2 [1 + b_2(\zeta - \zeta_2)^2]^{1/2}}{d_1 [1 + b_1(\zeta - \zeta_1)^2]^{1/2}}. \quad (4)$$

For $(\zeta - \zeta_{1,2})^2 \gg 1/b_{1,2}$, $\Lambda(\zeta)$ tends to the asymptotic value $\Lambda_\infty = [1/\Lambda(0)][(1 + 4\gamma_2)/(1 + 4\gamma_1)]^{1/2} [(1 + b_2 \zeta_2^2)/(1 + b_1 \zeta_1^2)]^{1/2}$ that depends on the input ellipticity (and eventually astigmatism) and the crystal temperature T . Whenever $[(1 + b_2 \zeta_2^2)/(1 + b_1 \zeta_1^2)]^{1/4} [(1 + 4\gamma_2)/(1 + 4\gamma_1)]^{1/4} = \Lambda(0)$, the input ellipticity is recovered and maintained as a result of the nonlinear interaction. From Eq. (3), it is also obvious that (2 + 1)D Gaussian diffusion-driven solitons (both cylindrical and elliptical) would be possible only when diffraction is isotropically compensated both in the x and y direction, that is, when both $\gamma_1 = -\frac{1}{4}$ and $\gamma_2 = -\frac{1}{4}$, a circumstance that requires $g_{11} = g_{12}$ (while, in general, $g_{11} > g_{12}$). Therefore, unlike the (1 + 1)D case [3], diffusion-driven scalar Gaussian solitons are not generally possible [13]. Note that when $d_1 = d_2$, our model predicts [see Eq. (4) and the expressions of $b_{1,2}$ after Eq. (3)] beam evolution toward an asymmetric Gaussian profile with ellipticity $\Lambda_\infty = [(1 + 4\gamma_2)/(1 + 4\gamma_1)]^{1/2}$, a signature of the strong anisotropy of the physical system.

Thus the first class of solutions describes analytically anomalous anisotropic self-induced diffraction and, in particular, allows for the description of the observed beam aspect ratio evolution.

The second class of solutions of Eq. (2), valid for $\gamma_1 < -\frac{1}{4}$ and $\gamma_2 < -\frac{1}{4}$ reads

$$A(\xi, \eta, \zeta) = A_0 \exp[-i(\alpha_1^2 \beta_1^2 + \alpha_2^2 \beta_2^2) \zeta] \times \left[\frac{1}{\cosh(\beta_1 \xi)} \right]^{\alpha_1^2} \left[\frac{1}{\cosh(\beta_2 \eta)} \right]^{\alpha_2^2}, \quad (5)$$

where $\alpha_1^2 = -1/(1 + 4\gamma_1)$, $\alpha_2^2 = -1/(1 + 4\gamma_2)$, and β_1 and β_2 are arbitrary parameters. This represents a class of non-Gaussian self-trapped solutions in the form of noncircular spatial solitons. These solutions, although feasible (unlike Gaussian solitons), have not been observed in KLTN (see discussion below). They are peculiar in that they do not obey any sort of light-dependent existence curve: They exist for arbitrary values of β_1 and β_2 and are determined solely by the actual proximity to the dielectric anomaly. They have no characteristic length scale. Stability analysis can be carried out along the lines introduced in Ref. [14], extending the 1D treatment to the 2D case considering the separability of Eq. (2). Thus, if l_p is the characteristic length scale of

TABLE I. Interferometrically measured values of γ_1 .

$T(^{\circ}\text{C}) \pm 0.2^{\circ}\text{C}$	10.2	10.5	11.0	11.5	12.0
$-\gamma_1 \pm 0.02$	0.17	0.09	0.06	0.04	0.03

the perturbation, and 1_x and 1_y are those of the soliton, stability can be demonstrated when $1_{x,y} \gg 1_p$. Solitons exist *only* when self-trapping is present in *both* transverse directions. Given β_1 and β_2 , the trapped ellipticity reflects the ratio of the strength of the nonlinearity in the two directions.

In order to test the quantitative agreement between theory and experiment we must evaluate the values of γ_1 and γ_2 as a function of T . The beam astigmatism was negligible in the (2 + 1)D configuration ($\xi_1 = \xi_2 = 0$). The principal dependence of the γ_i ($i = 1, 2$) on temperature is through ϵ_r that is greatly enhanced as the temperature is lowered towards T_c . In the proximity of the phase transition, the bulk dielectric crystal response is smeared out by the temperature gradient and other large-scale crystal inhomogeneities, and values of ϵ_r will in general be far lower than actual “local” crystal values. For temperatures where these effects have a negligible effect ($T > 12^{\circ}\text{C}$ with our setup) we are able to fit bulk ϵ_r values with the Curie-Weiss law, with $C = 1.3 \times 10^5 (^{\circ}\text{C})$ and $T_0 = 6.2^{\circ}\text{C}$. The peak value of ϵ_r actually measured directly (in the capacitance experiment) was approximately 3×10^4 . For values of T closer to T_c we directly measured the local (for the transverse regions of about $200 \times 200 \mu\text{m}^2$) electro-optic index modulation by inserting the sample in one arm of a Mach-Zehnder interferometer. With the polarization parallel to the applied external field, the measurements allowed the evaluation of γ_1 : With the polarization orthogonal to the applied field we determined the value of γ_2 . In the out-of-transition range, this allows also a measurement of $g_{11} = 0.12 \text{ m}^4 \text{ C}^{-2}$ and $g_{12} = 0.02 \text{ m}^4 \text{ C}^{-2}$ (having independently measured ϵ_r). Measured values of γ_1 are listed in Table I for near-transition temperatures. The listed values are higher than those expected from the Curie-Weiss relationship, and this can be phenomenologically attributed to an increase in the value of g_{11} , as the quadratic dependence of Δn still held for low applied voltages ($V < 250 \text{ V}$). Values of γ_2 , were such as to induce no appreciable diffusion-driven effects, remained always more than 5 times smaller (in absolute value) than the corresponding values of γ_1 for the temperatures investigated. In Fig. 2 the solid curve represents the theoretical curve obtained from Table I for the (1 + 1)D case [i.e., Eq. (3) with $d_2 \rightarrow \infty$]. The quantitative agreement is satisfactory, although the strong focusing for temperatures very near T_c may indicate that here some different mechanism is playing an important role. For ellipticity recovery in the (2 + 1)D case we recover the input ellipticity $\Lambda(0) = 1.5$ at $T = 10.2^{\circ}\text{C}$ (see Fig. 3). Our theory predicts that the “recoverable” ellipticity at this tempera-

ture is $\Lambda_{\text{theor}} = 1.3$, being $\gamma_1 = -0.17$ (see Table I) and $|\gamma_2| \ll 1$. Thus again, as in the (1 + 1)D case, the nonlinear response is stronger than expected.

Our model neglects, with respect to the peak intensity I_0 , the dark irradiance intensity I_d associated with crystal thermal carrier excitation and spurious background illumination. In order to evaluate the influence of the beam tails, where I is inevitably comparable with I_d , we have performed a numerical (1 + 1)D propagation (i.e., $d_2 \rightarrow \infty$). No appreciable differences exist between analytic and numerical solutions over many diffraction lengths.

Regarding the possibility of observing noncircular diffusion-driven solitons, our samples of KLTN do not support a sufficiently strong dielectric anomaly. The mechanism is however not peculiar to KLTN, and stronger anomalies have been reported in different ferroelectrics, such as strontium-barium-niobate and antimony sulphoide [11]. In these materials at least (1 + 1)D solitons should be attainable.

In conclusion, we have experimentally and theoretically investigated self-induced anomalies in optical beam diffraction in an anisotropic diffusion-type nonlinearity. The system studied, a doped ferroelectric heated above the Curie temperature, is described by a higher-order logarithmic nonlinearity and allows the analytical description of strong nonlinear propagation effects, such as intensity independent self-focusing and diffractive beam aspect ratio recovery and conservation. Furthermore, it allows us to predict noncircular solitons with no characteristic length scale.

We thank M. Segev for many helpful discussions. E. D.’s work was in collaboration with the Italian Communications Administration.

-
- [1] M. Segev and A. Agranat, *Opt. Lett.* **22**, 1299 (1997).
 - [2] E. DelRe, B. Crosignani, M. Tamburrini, M. Segev, M. Mitchell, E. Refaeli, and A. Agranat, *Opt. Lett.* **23**, 421 (1998).
 - [3] B. Crosignani, E. DelRe, P. Di Porto, and A. Degasperis, *Opt. Lett.* **23**, 912 (1998).
 - [4] D. Christodoulides and T. Coskun, *Opt. Lett.* **21**, 1460 (1996); A. Zozulya, M. Saffman, and D. Anderson, *Phys. Rev. Lett.* **73**, 818 (1994).
 - [5] R. A. Fuerst, B. L. Lawrence, W. E. Torruellas, and G. I. Stegeman, *Opt. Lett.* **22**, 19 (1997).
 - [6] A. W. Snyder and J. D. Mitchell, *Opt. Lett.* **22**, 16 (1997).
 - [7] V. Tikhonenko, *Opt. Lett.* **23**, 594 (1998).
 - [8] A. W. Snyder and D. J. Mitchell, *Phys. Rev. Lett.* **80**, 1422 (1998).
 - [9] B. Crosignani *et al.*, *J. Opt. Soc. Am. B* **14**, 3078 (1997).
 - [10] Linearity is valid in absence of spontaneous phenomena.
 - [11] Y. Xu, *Ferroelectric Materials and Their Applications* (North-Holland, Amsterdam, 1991).
 - [12] A. Yariv and P. Yeh, *Optical Waves in Crystals* (Wiley, New York, 1984).
 - [13] Beam polarization introduces a privileged axis.
 - [14] M. Segev, B. Crosignani, P. Di Porto, A. Yariv, G. Duree, G. Salamo, and E. Sharp, *Opt. Lett.* **19**, 1296 (1994).